

# Effect of Plastic Deformation on Elastic Properties of Austenitic Steel at Different Temperatures

*Vyacheslav Klyushnikov\**

Federal Research Center Institute of Applied Physics of the Russian Academy of Sciences, 603024, 85, Belinskogo str., Nizhny Novgorod, Russia

**Abstract.** Plastic deformation of austenitic steel AISI 321 at various temperatures was carried out. The temperature dependences of the elastic characteristics of the material have been studied. A difference between the dependences of elastic wave velocities and acoustic birefringence parameter is found at different deformation temperatures. The effect of texture changes and martensitic transformation on the studied elastic parameters is considered. It is found that the birefringence parameter changes non-monotonically upon deformation at 20°C and 40°C, and monotonically at 60°C. It is shown that the difference in the nature of the change is due to the intensity of the martensitic transformation.

## Introduction

It is known that phase changes occur in chromium-nickel steels with low stacking fault energy during plastic deformation in addition to the process of microdamages accumulation [1, 2]. Mainly, these changes is the formation from the paramagnetic austenite (face-centered cubic lattice) to the ferromagnetic  $\alpha'$ -martensite (body-centered tetragonal lattice).

The intensity of the martensitic transformation and the volume fraction  $\alpha'$ -martensite depends on the stressed-deformed state of a material, the rate and temperature of deformation [3–9], the chemical composition, and the stacking fault energy [9-12].

The accumulation of damage is in the material in addition to the phase formation during plastic deformation. These two processes can be considered to have a decisive influence on the elastic and electromagnetic properties of the material

Changes in the elastic modulus of the entire material due to the allocation of an additional phase can be taken into account using different approximations. For example, the determination of modules of material, comprised of isotropic phases, is carried out using the Voigt and Reuss approximations:

$$M_C = \sum_{i=1}^N M_i v_i, \frac{1}{M_C} = \sum_{i=1}^N \frac{v_i}{M_i}, \quad (1)$$

---

\* Corresponding author: [slavchuk2@yandex.ru](mailto:slavchuk2@yandex.ru)

where  $M_c$  – the modulus of elasticity of the entire material,  $M_i$  и  $v_i$  – elastic modulus and volume content of each phase, respectively,  $N$  – number of phases

Approximations of Voigt and Reuss represent rigorous upper and lower bounds on the elastic modulus for multiphase materials.

The relation between the stiffness constant and velocities  $V_{33}$  of the longitudinal wave and  $V_{31}$  and  $V_{32}$  of the shear waves [13] propagating in an orthotropic material can be written in the form:

$$V_{33} = \sqrt{c_{33}/\rho}, V_{31} = \sqrt{c_{55}/\rho}, V_{32} = \sqrt{c_{44}/\rho}, \quad (2)$$

where  $\rho$  – is the density of the material. The first subscript on V indicates the direction of propagation of the wave and the second subscript indicates the polarization.

In the presence of the elastic properties anisotropy of the material, the velocities of shear waves polarized along and across the anisotropy axes, differ. To determine the degree of anisotropy, the acoustic birefringence parameter  $B$  is used, which is expressed in terms of the stiffness constant as follows:

$$B = \frac{c_{55}-c_{44}}{c_{55}+c_{44}}, \quad (3)$$

For an isotropic material ( $c_{44}=c_{55}=\mu$ ,  $\mu$  – shear modulus)  $B=0$ .

The change in  $c_{33}/c_{44}$  and  $c_{33}/c_{55}$  also characterizes the development of elastic properties anisotropy during force loading [13, 14]. In particular,  $\Delta(c_{33}/c_{44})$  is sensitive to the strain amplitude under fatigue loading was found.

It is known that the change in the anisotropy of the materials properties during plastic deformation depends on the type of crystal lattice. In the [15] it is shown that due to the difference in sliding systems, the acoustic anisotropy of face-centered cubic (FCC) metals decreases during plastic deformation, and metals with face-centered cubic (BCC) structure increases. The rate of acoustic birefringence change is significantly affected by the scattering of the original texture. Accordingly, plastic deformation of austenite should reduce the acoustic anisotropy of the entire material, but the formation and deformation of the  $\alpha'$ -martensite should increase it.

Earlier studies [3, 16, 17] have shown that the higher the plastic deformation temperature, the less martensite phase is formation. Accordingly, the elastic waves velocity is more influenced by damage, which accumulates in the initial phase of austenite. One of the most important parameters determining the martensitic transformation is the temperature  $M_d$  at which 50% of  $\alpha'$ -martensite is formation after deformation of 30%. The correlation of  $M_d$  with the chemical composition of steels was experimentally obtained in [3]:

$$M_d(30/50)(^\circ\text{C})= 413-13.7(\%\text{Cr})-9.5(\%\text{Ni})-8.1(\%\text{Mn})-18.5(\%\text{Mo})-9.2(\%\text{Si})-462(\%[\text{C}+\text{N}]) \quad (4)$$

where (%) refers to the atomic weight percentage of each element in the steel.

In this paper, the influence of the plastic deformation temperature on the elastic properties of austenitic steel AISI 321 and the formation of the  $\alpha'$ -martensite was investigated.

The effect of damage associated with decompression of the material  $\psi$  on the bulk modulus  $K$  and shear modulus  $\mu$  can be expressed as follows:

$$K=K_0+k_1\psi; \mu=\mu_0+k_2\psi \quad (5)$$

where  $k_1$  и  $k_2$  – coefficients,  $K_0$  и  $\mu_0$  – the initial the bulk modulus and the shear modulus, respectively.

To determine the damage  $\psi$ , the density of the initial material  $\rho_0$  and the density of the material after destruction  $\rho$  were measured:

$$\psi = (\rho_0 - \rho) / \rho_0 \tag{6}$$

To determine the elastic moduli using the echo-pulse method, the propagation velocities of longitudinal and shear ultrasonic waves were measured. The amount of the  $\alpha'$ -martensite was controlled by the eddy current method.

### Experimental procedure

The material investigated was metastable austenitic stainless steel AISI 321 in as-received condition. The chemical composition is shown in Table 1. The cylindrical specimens with plane parallel platforms cut on both sides of the working zone for ultrasonic and eddy-current measurements were used, Fig.1.

**Table 1.** Chemical composition of investigated steel AISI 321, %.

| C    | Cr    | Ni   | Mn   | Mo   | Ti   | P     | S     | Si   | Fe      |
|------|-------|------|------|------|------|-------|-------|------|---------|
| 0.03 | 17.27 | 9.02 | 0.56 | 0.22 | 0.31 | 0.029 | 0.003 | 0.43 | balance |

The uniaxial tension was carried out step-by-step with the strain rate  $1 \cdot 10^{-3} \text{ s}^{-1}$  using a BISS Nano UT-01-0025 servo-hydraulic testing machine. The ultrasonic studies and analysis of changes of the magnetic properties governed by the formation of the magnetic  $\alpha'$ -martensite were implemented before testing and after each step. Test temperature was 20°C, 40°C and 60°C.

To measure the time of propagation of the shear and longitudinal elastic waves, the echo-pulse method was used, utilizing the broadband acoustic transducers Olympus V156-RM (shear wave) and Olympus V110-RM (longitudinal wave). The central frequency of the piezoelectric transducers (PZT) was  $\sim 5 \text{ MHz}$ , their diameter was 6 mm. A commercially available ultrasonic flaw detector (model A1212 MASTER), digital oscilloscope (model LA-n10USB) and PC were used for ultrasonic measurements. Sampling frequency of the oscilloscope was 100 MHz. Longitudinal and shear waves propagated along the Z(3) axis (Fig. 1); the polarization of shear waves was along the loading axis X(1); in the next test, it was along the axis Y(2).

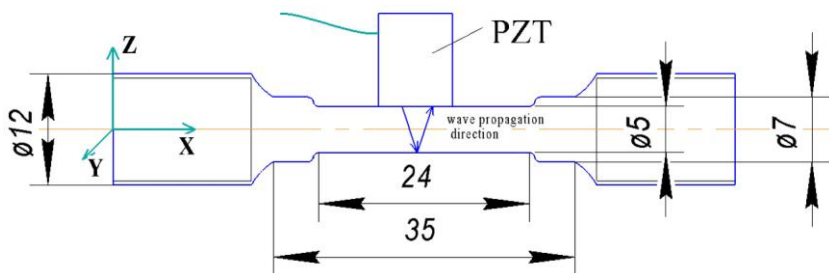


**Fig.1.** Tensile specimens geometry.

The amplitude-time diagram of echo pulses series for longitudinal and shear elastic waves was recorded in each zone. The time of flight of the ultrasonic wave was measured

between the first and third echo pulses. Next, acoustic birefringence parameter was defined in terms of times of flight of two orthogonally polarized shear waves as:

$$B = 2 \frac{t_{32} - t_{31}}{t_{32} + t_{31}} \quad (7)$$

where times of flight of two shear waves with mutually orthogonal polarizations along and across loading axis X and propagated along Z.

To determine the density of steel, the method of hydrostatic weighing was used. The density of a material is determined by weighing it twice, first in air and then in a liquid whose density is known (usually in distilled water). At the first weighing, the body weight is determined, by the difference in the results of both weighings – its volume. Hydrostatic weighing was carried out using an AB60-01 analytical balance corresponding to I (special) accuracy class according to GOST 24104-2001 [18].

Steel density  $\rho_{st}$  was determined by the formula:

$$\rho_{st} = \frac{m_{air}}{m_{air} - m_w} (\rho_w - \rho_{air}) + \rho_{air} \quad (8)$$

where  $m_{air}$ ,  $m_w$  is the mass of the sample in air and water, respectively,  $\rho_w = 1 \text{ g/cm}^3$  – density distilled water,  $\rho_{air} = 0.0012 \text{ g/cm}^3$  – density air. Density measurements were taken five times with error  $0.005 \text{ g/cm}^3$ .

The density was determined on fragments of material cut from the deformation zone of the samples in such a way that the macro crack (the appearance of which indicated destruction) was outside the fragments.

To calculate the Young's modulus  $E$  and the shear modulus  $\mu$  before and after deformation of the material expressions for the isotropic approximation were used:

$$\mu = \rho V_\tau^2, \quad E = \rho V_l^2 \frac{(1+\nu)(1-2\nu)}{1-\nu} \quad (9)$$

where  $\nu$  – Poisson's ratio,  $V_l$  – velocity of longitudinal elastic waves,  $V_\tau$  – is averaged values  $V_{31}$  and  $V_{32}$ . Poisson's ratio  $\nu$  is defined as:

$$\nu = \frac{V_l^2 - 2V_\tau^2}{2(V_l^2 - V_\tau^2)} \quad (10)$$

As a result of processing of the obtained data, the propagation time of the elastic wave was found and the velocities were calculated; the errors were about 3 ns and 5 m/s, respectively

A multifunction eddy current instrument MVP-2M (Scientific-Production Center "Kropus" Ltd., Russia) with an absolute probe operating at 1 kHz was used for the eddy current studies. This instrument can measure the added voltage of eddy current probe and the percentage the fraction of the ferromagnetic phase (%-ferrite). Originally it was developed for the determination of the ferrite in austenitic materials. The device was calibrated with ferrite samples by the manufacturer. The calibration curve determining the relationship between the added voltage of eddy current probe and ferromagnetic phase (%-ferrite) was added to the device firmware by the manufacturer.

## Results and discussion

The volume fraction of strain-induced  $\alpha'$ -martensite in the early stages of plastic loading increases slightly, Fig. 2. However, when the deformation value of about 25% is reached, a drastically increase in the volume fraction of the martensite phase is observed. It should be noted that during plastic deformation at a temperature of 60°C, the intensity of the strain-induced martensite is not as high as at other temperatures. The  $M_d$  temperature was 68°C according to the formula (4).

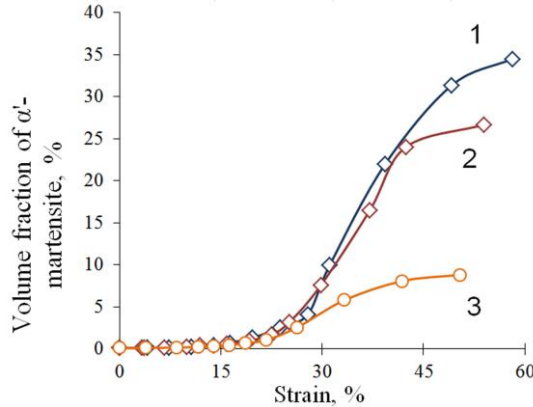


**Fig. 2.** The volume fraction of strain-induced  $\alpha'$ -martensite as a function of plastic strain.

Various changes in the volume fraction of  $\alpha'$ -martensite affected the density of the material during plastic deformation. So, at the deformation temperature  $T = 20^\circ\text{C}$ , the decompression was 2.3%, at  $T = 40^\circ\text{C} - 1.6\%$  at  $T = 60^\circ\text{C} - 0.8\%$ .

The change in the velocity  $V_{32}$  is monotonic, while the change of velocity  $V_{31}$  nonmonotonic, Fig.3.

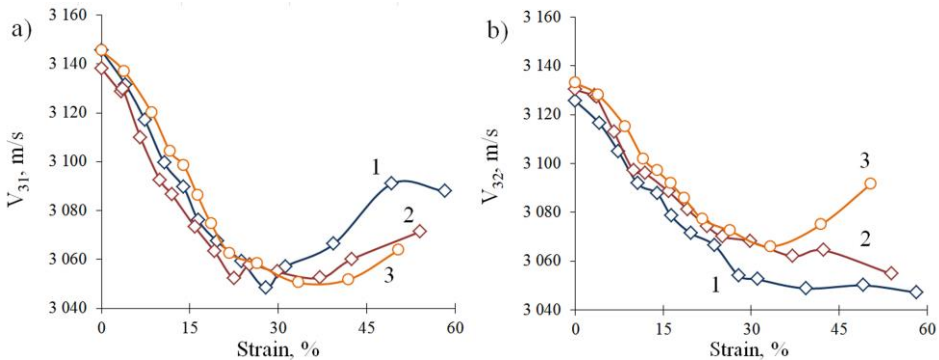


**Fig.3.** Temperature dependences velocity of shear waves  $V_{31}$  (a) and  $V_{32}$  (b) on the plastic strain at deformation temperature 20°C (1), 40°C (2) and 60°C (3).

Apparently, with the increase of deformation, the elastic modulus and density of the material change in such a way that at the initial stage of deformation their ratio, which determines the velocity of shear waves, decreases. However, when the same strain value is reached (as in Fig.3a), the velocity  $V_{31}$  increases. This appears to be due to the accumulation of the volume fraction of strain-induced martensite and its location in the structure of the material.

Young's modulus and shear modulus of the material before and after loading at different temperatures, calculated by the formula 9, are shown in the table 2.

**Table 2.** Young's modulus, shear modulus and density material before and after loading

|                  | Density, [g/cm <sup>3</sup> ] | $\mu$ , [GPa] | $E$ , [GPa] |
|------------------|-------------------------------|---------------|-------------|
| Initial material | 7.919                         | 77.9          | 201         |
| 20°C             | 7.740                         | 72.8          | 190         |
| 40°C             | 7.788                         | 73.1          | 191         |
| 60°C             | 7.853                         | 74.9          | 195         |

The study of the anisotropy of elastic properties showed that  $\Delta(c_{33}/c_{44})$  and  $\Delta(c_{33}/c_{55})$  at the early stage of deformation change in the same way regardless of the loading temperature, Fig.4.

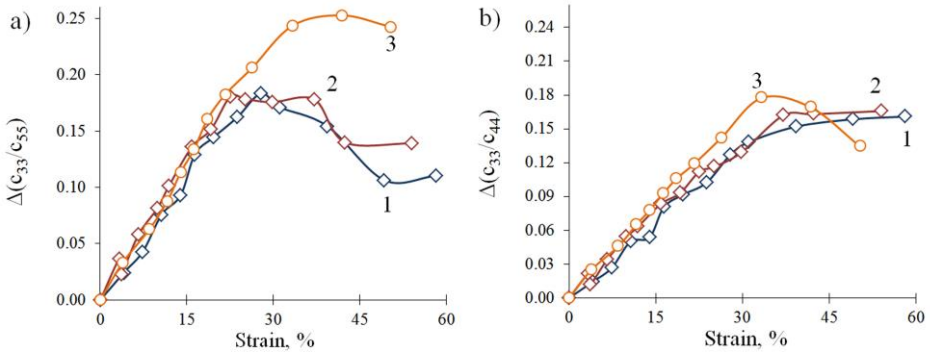


**Fig.4.** Evolution  $\Delta(c_{33}/c_{55})$  (a) and  $\Delta(c_{33}/c_{44})$  (b) during plastic deformation at temperature 20°C (1), 40°C (2) and 60°C (3).

The similar pattern is manifested for the dependence of the change in the acoustic birefringence parameter  $B$  on the plastic deformation (Fig.5).

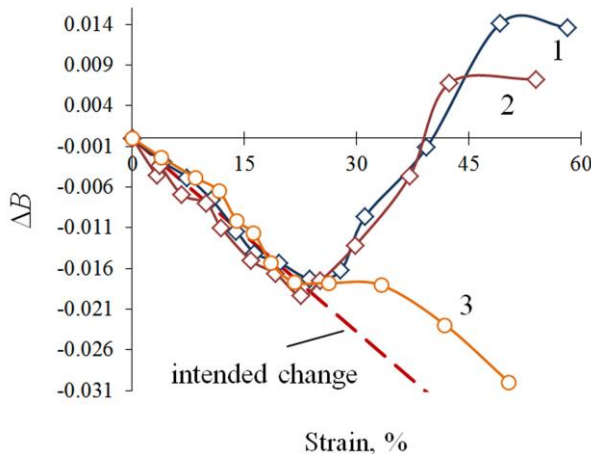


**Fig. 5.** Dependence of change in the acoustic birefringence parameter  $B$  on the plastic strain at deformation temperature 20°C (1), 40°C (2) and 60°C (3).

It is assumed that at the initial stage of uniaxial tension the texture change is more influenced by the process of austenite deformation than the martensitic formation. At the initial stage of deformation, the birefringence parameter decreases, since austenite with a FCC lattice prevails in the material. With further deformation at temperatures of 20°C and 40°C, the formation of a phase with a BCC lattice occurs more intensively, which leads to an increase in the birefringence parameter. This means that the formation of  $\alpha'$ -martensite began to affect the texture change more than the process of austenite deformation. When deformed at a temperature of 60°C, the  $\alpha'$ -martensite phase is formed less intensively and the velocity, parameters  $B$ ,  $c_{33}/c_{44}$  and  $c_{33}/c_{55}$  are affected by damage in the initial phase of austenite. An example of a sample with a temperature of 60°C shows the expected development of parameter  $B$  in the absence of martensitic transformation in the material.

## Conclusion

Effect of plastic deformation on elastic properties of austenitic steel at different temperatures was studied. The Young's modulus and the shear modulus of the steel material before and after destruction are obtained.

At deformation up to 25%, the volume fraction of  $\alpha'$ -martensite increased slightly. Thus, the elastic characteristics are mainly affected by the damage accumulation, the birefringence parameter decreases, and changes in  $c_{33}/c_{44}$  and  $c_{33}/c_{55}$  change in the same way regardless of the loading temperature.

With further deformation at temperatures of 20 °C and 40 °C, the formation of the  $\alpha'$ -martensite phase with a BCC lattice occurs more intensively and affects the texture change to a greater extent than the process of austenite deformation. This is appeared in the evolution of elastic parameters in the process of plastic deformation. At deformation with temperature of 60°C, the  $\alpha'$ -martensite is formed less intensively. There is a difference in the change of elastic parameters depending on the deformation temperature.

The obtained dependences reflect the combined effect of martensite transformation and damage accumulation at different temperature of plastic deformation steel AISI 321.

This work was supported by the Russian Scientific Foundation (project No 22-29-01237).

## References

1. P. L. Mangonon, G. Thomas, The martensite phases in 304 Stainless Steel, Metall Mater Trans B. 1 (1970) 1577-1586.
2. J. Singh, Influence of deformation on the transformation of austenitic stainless steels, J. Mat. Sc. 20 (1985) 3157-3166.
3. T.J. Angel, Formation of martensite in austenitic stainless steels, J. Iron Steel Inst. 177 (1954) 165–174.
4. G. W. Powell, E. R. Marshall, W. A. Backofen, Strain hardening of austenitic stainless steel, Trans. of the ASM. 50 (1958) 478-497.
5. S. S. Hecker, M. G. Stout, K. P. Staudhammer, J. L. Smith, Effects of strain state and strain rate on deformation induced transformation in 304 stainless steel: part I. Magnetic measurements and mechanical behavior, Metall. Trans. A. 13 (1982) 619 - 626.
6. G. L. Huang, D. K. Matlock, G. Krauss, Martensite formation, strain rate sensitivity and deformation behavior of type 304 austenitic steel sheet, Metall. Trans. A. 20A (1989) 1239-1246.
7. J. Talonen, P. Nenonen, G. Pape, H. Hanninen, Effect of strain rate on the strain-induced  $\gamma \rightarrow \alpha'$  martensite transformation and mechanical properties of austenitic stainless steels, Metall. Mater. Trans. A. 36A(2005) 421- 432.

8. J. A. Lichtenfeld, M. C. Mataya, C. J. van Tyne, Effect of strain rate on stress-strain behavior of alloy 309 and 304L austenitic stainless steel, *Metall. Mater. Trans. A.* 37(2006) 147–161.
9. A. F. Padilha, P. R. Rios, Decomposition of austenite in stainless steel, *ISIJ International.* 42 (2002) 325-337.
10. F. Lecroisey, A. Pineau, Martensitic transformations induced by plastic deformation in the Fe-Ni-Cr-C system, *Metall Trans. A.* 3 (1972) 387-396.
11. J.-Y. Choi, W. Jin, Strain induced martensite formation and its effect on strain hardening behavior in the cold drawn 304 austenitic stainless steels, *Scripta Mater.* 36(1997) 99-104.
12. G. B. Olson, M. Cohen, Kinetics of strain-induced martensitic nucleation, *Metall. Trans. A.* 6A (1975) 791-795.
13. A. V. Gonchar, V. V. Mishakin, V. A. Klyushnikov, K. V. Kurashkin Variation of elastic characteristics of metastable austenite steel under cycling straining, *Tech. Physics.* 62 (2017) 537–541.
14. V. Mishakin, A. Gonchar, V. Klyushnikov, K. Kurashkin, A. Fomin, O. Sergeeva, Monitoring the state of stainless steel under cyclic deformation by the acoustic and eddy current methods, *Meas. tech.* 64 (2021) 145-150.
15. K. V. Kurashkin, V. V. Mishakin, S. V. Kirikov, A. V. Gonchar, V. A. Klyushnikov Change in texture-dependent acoustic birefringence in  $\alpha$ -Fe and  $\gamma$ -Fe polycrystalline aggregates due to plastic deformation, *Phys. Mesomech.* 25 (2022) 80–84.
16. T. S. Byun, H. Naoyuki, K. Farrell. Temperature dependence of strain hardening and plastic instability behaviors in austenitic stainless steels, *Acta Mater.* 52 (2004) 3889-3899.
17. K. Mumtaz, S. Takahashi, J. Echigoya, L. Zhang, Y. Kamada, M. Sato, Temperature dependence of martensitic transformation in austenitic stainless steel, *J. Mat. Sc. Let.* 22 (2003) 423–427.
18. GOST R 24104-2001. Laboratory scales. General technical requirements. 2002–01–07. Moscow: Standartinform, 2007.